© ESO 2012

Evidence for enhanced chromospheric Ca II H & K emission in stars with close-in extrasolar planets

T. Krejčová[1] and J. Budaj[2]

[1] Department of Theoretical Physics and Astrophysics, Masaryk University, Kotlářská 2, 61137 Brno, Czech Republic
e-mail: terak@physics.muni.cz

[2] Astronomical Institute, Slovak Academy of Sciences, 05960 Tatranská Lomnica, Slovak Republic
e-mail: budaj@ta3.sk

ABSTRACT

Context. The planet-star interaction is manifested in many ways. It was found out that a close-in exoplanet causes small but measurable variability in the cores of a few lines in the spectra of several stars which corresponds to the orbital period of the exoplanet. Stars with and without exoplanets may have different properties.

Aims. The main goal of our study is to search for influence which exoplanets might have on atmospheres of their host stars. Unlike the previous studies, we do not study changes in the spectrum of a host star or differences between stars with and without exoplanets. We aim to study a large number of stars with exoplanets, current level of their chromospheric activity and look for a possible correlation with the exoplanetary properties.

Methods. To analyse the chromospheric activity of stars we exploit our own⋆ and publicly available archival spectra⋆⋆, measure the equivalent widths of the cores of Ca II H and K lines and use them as a tracer of their activity. Subsequently, we search for their dependence on the orbital parameters and mass of the exoplanet.

Results. We found a statistically significant evidence that the equivalent width of the Ca II K line emission and $\log R'_{HK}$ activity parameter of the host star varies with the semi-major axis and mass of the exoplanet. Stars with $T_{eff} \leq 5500$ K having exoplanets with semi-major axis $a \leq 0.15$ AU ($P_{orb} \leq 20$ days) have a broad range of Ca II K emissions and much stronger emission in general than stars at similar temperatures but with higher values of semi-major axes. Ca II K emission of cold stars ($T_{eff} \leq 5500$ K) with close-in exoplanets ($a \leq 0.15$ AU) is also more pronounced for more massive exoplanets.

Conclusions. The overall level of the chromospheric activity of stars may be affected by their close-in exoplanets. Stars with massive close-in exoplanets may be more active.

Key words. Planets and satellites: general – Planets and satellites: magnetic fields – Planet-star interactions – Stars: chromospheres – Stars: magnetic field – (Stars): planetary systems

1. Introduction

There is a wide variety of interactions which may occur between a close-in planet and its host star: evaporation of the planet (Vidal-Madjar et al. 2003; Hubbard et al. 2007), precession of the periastron due to the general relativity, tides or other planets (Jordán & Bakos 2008), synchronization and circularization of the planet's rotation and orbit, strong irradiation of the planet and its effect on the planet radius (Guillot & Showman 2002; Burrows et al. 2007), atmosphere or stratosphere (Hubeny et al. 2003; Burrows et al. 2008; Fortney et al. 2008). However, not only the planet suffers from this interaction. Hot Jupiters also rise strong tides on their parent stars and some of the stars can become synchronized as well. Dissipation of the tides can lead to an extra heating of the stellar atmosphere. Magnetic field of the exoplanet may interact with the stellar magnetic structures in a very complicated manner which is not very well understood and is a subject of recent studies (Cuntz et al. 2000; Rubenstein & Schaefer 2000; Ip et al. 2004; Lanza 2008). Such

type of interaction might be observed mainly in the chromospheres and coronae of the parent stars.

The planet-star interaction is currently examined across the whole energy spectrum beginning from X-rays to the radio waves and from the ground as well as from the space. A planet-induced X-ray emission in the system HD179949 was observed by Saar et al. (2008). On the other hand, the search for correlation between X-ray luminosity and exoplanetary parameters (Kashyap et al. 2008; Poppenhaeger & Schmitt 2011) revealed quite contradictory results. Based on the observations in the optical region, Shkolnik et al. (2005, 2008) discovered variability in the cores of Ca II H & K, Hα and Ca II IR triplet in a few exoplanet host stars induced by the exoplanet.

Ca II H & K lines (3933.7 and 3968.5 Å) are one of the best indicators of stellar activity observable from the ground (Wilson 1968). These lines are very strong and their core is formed in the chromosphere of the star. For quantitative assessment of chromospheric activity of stars of different spectral types, the chromosphere emission ratio $\log R'_{HK}$ (the ratio of the emission from the chromosphere in the cores of the Ca II H & K lines to the total bolometric emission of the star) was introduced by Noyes et al. (1984). Large $\log R'_{HK}$ values mean higher activity.

Knutson et al. (2010) found a correlation between the presence of the exoplanetary stratosphere and the Ca II H & K ac-
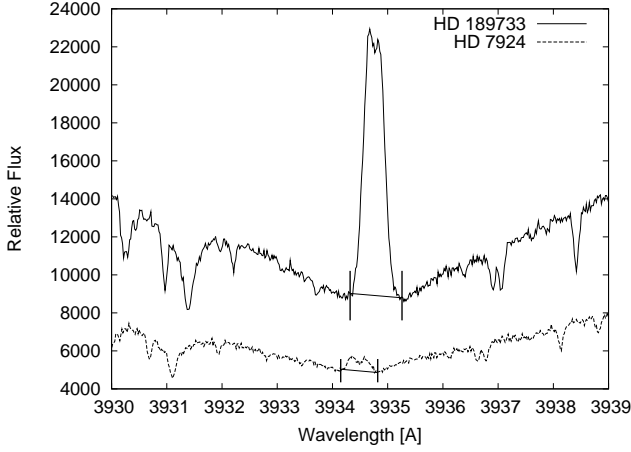

Fig. 1. Illustration of the Ca II K line in two different stars. We measured only the equivalent width of core of the line with the central reversal. By definition, EQW is negative for emission and positive for absorption.

tivity index $\log R'_{HK}$ of the star. Consequently, Hartman (2010) found a correlation between the surface gravity of Hot Jupiters and the stellar activity.

Recently, Canto Martins et al. (2011) analysed the sample of stars with and without extrasolar planets. They searched for a correlation between planetary parameters and the $\log R'_{HK}$ parameter but didn't reveal any convincing proof for enhanced planet-induced activity in the chromosphere of the stars. On the other hand, Gonzalez (2011) claims that stars with exoplanets have smaller $v \sin i$ and $\log R'_{HK}$ values (i.e. less activity) than stars without exoplanets.

In this paper, we search for possible correlations between chromospheric activity of the star and properties of exoplanets. The equivalent width (hereafter EQW) of Ca II K line emission is used as an indicator of the level of chromospheric activity of the parent star.

2. Observation & Data

Stellar spectra used in our analysis originate from two different sources. The main source is the publicly available Keck HIRES spectrograph archive. These spectra have a typical resolution of up to 85 000. We carefully selected only those spectra with the signal-to-noise ratio high enough to measure the precise EQW of Ca II K emission.

These data were accompanied by our own observations of several stars (HD 179949, HD 212301, HD 149143 and Wasp-18) with close-in exoplanet. We obtained these data with FEROS spectrograph mounted on 2.2 m ESO/MPG telescope (night 18/19.9.2010). Spectra were reduced with standard procedure using IRAF package[1]. These data are marked in all plots as red squares. We measured the EQW (in Å) of the central reversal in the core of Ca II K from all spectra using IRAF (see Figure 1). This plot illustrates a placement of the pseudocontinuum in our measurements. Advantage of using such simple EQW measurements is that they are defined on a short spectral interval which is about 1 Å wide. Consequently, they are not very sensitive to various calibrations (continuum rectification, blaze function removal) inherent in the echelle spectroscopy. For comparison, $\log R'_{HK}$ index relies on the information from four spectral
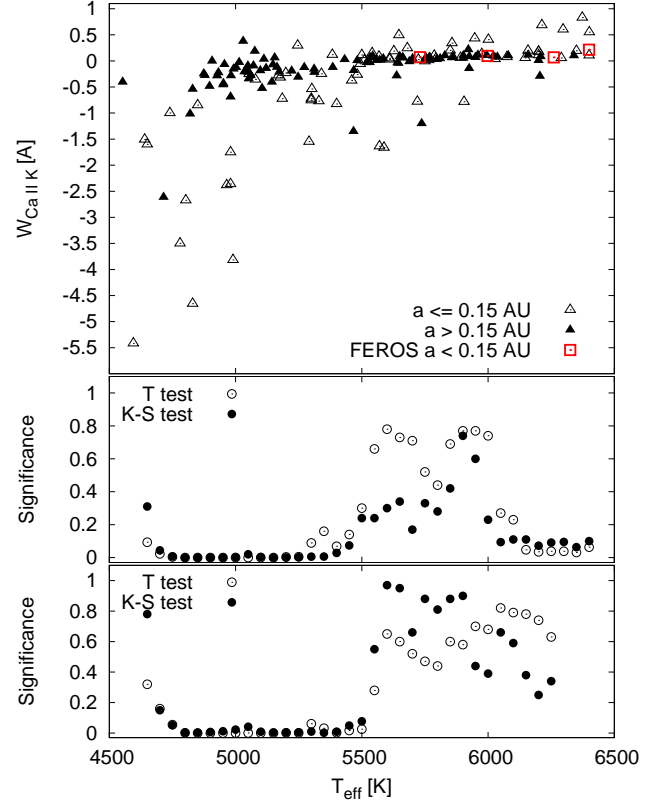
[1] http://iraf.noao.edu/

Fig. 2. *Top*: Dependence of the equivalent width of the Ca II K emission on temperature of the parent star. Emission and chromospheric activity increase with decreasing temperature. Cooler stars ($T_{eff} \leq 5\,500$ K) with close-in planets are more active than stars with more distant planets. Empty triangles are exoplanetary systems with $a \leq 0.15$ AU, full triangles are systems with $a > 0.15$ AU and red squares are our data from FEROS. *Middle*: Statistical Student's *t*-test (empty circles) and Kolmogorov-Smirnov test (full circles) show whether the two distributions are the same. Low probability values for $T_{eff} \leq 5\,500$ K mean a significant evidence that the chromospheric activity of stars with close-in planets is different from that of stars with distant planets. *Bottom*: The same statistical tests performed on systems discovered by RV technique only.

channels covering about 100 Å wide interval. If extracted from echelle spectra it is much more sensitive to a proper flux calibration and subject to added uncertainties.

The sample of the data contains 206+4 stars with extrasolar planets in the temperature range from approx. 4 500 to 6 600 K. The semi-major axes of the exoplanets lie in the interval 0.016–5.15 AU. Table 1 lists the parameters of exoplanetary systems used in the study.

For comparison with our EQW values, we also used the parameter $\log R'_{HK}$ taken from the work of Wright et al. (2004), Knutson et al. (2010) and Isaacson & Fischer (2010).

3. Statistical analysis and results

We will start by exploring the dependence of the EQW of Ca II K emission on the effective temperature of the star. This is illus-
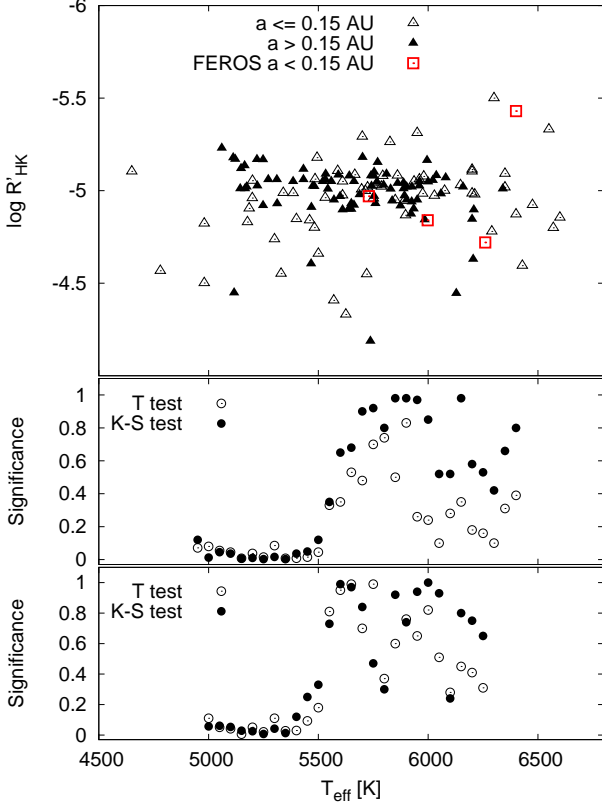
Fig. 3. *Top*: Dependence of the activity index $\log R'_{HK}$ on temperature of the parent star. Emission and chromospheric activity increase with decreasing temperature. Cooler stars ($T_{eff} \leq 5\,500$ K) with close-in planets are more active than stars with more distant planets. Empty triangles are exoplanetary systems with $a \leq 0.15$ AU, full triangles are systems with $a > 0.15$ AU and red squares are our data from FEROS. *Middle*: Statistical Student's t-test (empty circles) and Kolmogorov-Smirnov test (full circles) show whether the two distributions are the same. Low probability values for $T_{eff} \leq 5\,500$ K mean a significant evidence that the chromospheric activity of stars with close-in planets is different from that of stars with distant planets. *Bottom*: The same statistical tests performed on systems discovered by RV technique only.

trated in the top panel of Figure 2[2]. One can see that the EQW decreases i.e. core emission increases towards lower temperatures. Part of the reason for this behaviour is that the photospheric flux at the core of the Ca II K line is lower for cooler stars than for hotter stars. At the same time, the data points which stand for stars with $T_{eff} > 5\,500$ K show only a narrow spread of Ca II K EQWs while cooler stars have a broad range of these values. This means that we should focus on the cooler stars.

In the next step, we will distinguish between the close-in and distant exoplanets. This is also shown in Figure 2 where planets with semi-major axis shorter/longer than 0.15 AU have different symbols. One can see that stars with close-in planets clearly tend to have higher Ca II K emission (lower EQWs) than stars with distant planets. To verify whether this finding is statistically significant, we performed two statistical tests on these two

data samples (close-in vs distant planets). The first one was the Student's t-test which determines whether the means of these two samples are equal. The other test was Kolmogorov-Smirnov test which we used to determine whether the two groups originate from the same population. We selected a running window which is 400 K wide and runs along the x-axis (temperature) with the step of 50 K. Consequently, we performed the statistical tests on the two samples of stars within the current window and plot the result versus the center of the current window. The middle panel of Figure 2 shows the resulting probability (as a function of temperature) that the two samples have the same mean or originate from the same population. Small value of probability means that the two samples are different. It can be seen (figure 2), that the difference between the stars with close-in and distant exoplanets is statistically significant for cooler stars with $T_{eff} \leq 5\,500$ K.

However, notice that while most of the distant exoplanets were discovered by the radial velocity (RV) measurements, many of the close-in planets were discovered by transits. The two techniques may have very different criteria for selection of the exoplanetary candidates and especially the RV measurements concentrate on low activity stars. That is why in the bottom panel of Figure 2, we included only the stars with exoplanets discovered by the RV technique into the statistics. On this reduced data sample we performed the same statistical tests as in the previous case – we chose the same size of the step and the running window. Even if the transit data are excluded, the tests show significant difference between the stars with close-in and distant exoplanets.

To verify the above mentioned trends, we also explored the $\log R'_{HK}$ parameter. This parameter does not show the strong temperature dependence (Figure 3). When we distinguish the stars with close-in exoplanets ($a \leq 0.15$ AU) from stars with distant exoplanets ($a > 0.15$ AU) using different symbols we observe the same tendency as before. Namely, stars with close-in planets show wider range of $\log R'_{HK}$ values than stars with distant planets. Cooler stars ($T_{eff} \leq 5\,500$ K) with close-in planets have higher values of $\log R'_{HK}$ and thus higher chromospheric activity.
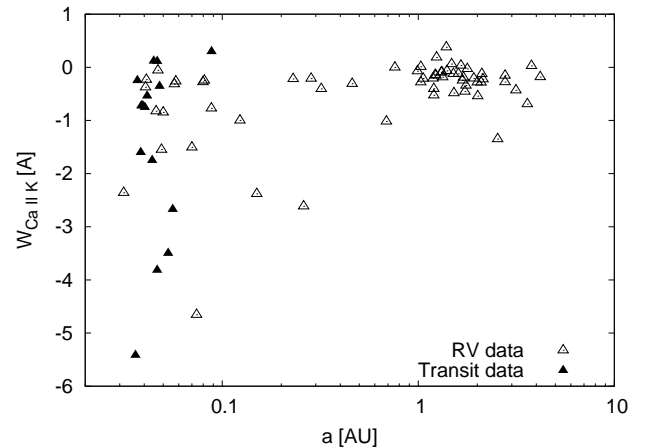
Fig. 4. Dependence of the equivalent width of Ca II K emission on the semi-major axis. Included are only systems with $T_{eff} \leq 5\,500$ K. Empty triangles are exoplanetary systems discovered by RV technique, full triangles are systems discovered by transit method. Cold stars with close-in planets ($a \leq 0.15$ AU) have higher scatter and a generally higher Ca II K emission than cold stars with distant planets. This does not apply to hotter stars.

---

[2] For comparison we also measured the Ca II H emission (figure 7 and 8). These are T_{eff} vs. W_{CaIIH} and semi-major axis vs. W_{CaIIH} plots.

3

Fig. 5. Dependence of the activity index $\log R'_{HK}$ on the semi-major axis. Triangles are exoplanetary systems discovered by RV technique, circles are systems discovered by transit method.

The difference between stars with close-in and distant planets is statistically significant for $T_{eff} \leq 5\,500\,K$ which is illustrated by the Student's t-test and Kolmogorov-Smirnov test in the middle panel of Figure 3. The bottom panel of the figure depicts the same tests applied to the systems discovered by the RV technique only and indicates that the difference is statistically significant even though the sample consists of stars with planets detected by a single technique. In this figure, we used the same kind of analysis within a running window as before.

It appears that the semi-major axis of the innermost planet around a star is in some way connected with the chromospheric activity of the star. So, in the next step, we explore the dependence of the activity on the semi-major axis a. This dependence is illustrated in Figure 4 which displays results we measured – EQW of Ca II K emission as a function of the semi-major axis. Following our findings above, we selected only systems with $T_{eff} \leq 5\,500\,K$. One can clearly see two distinctive populations there. Stars with close-in exoplanets with $a \leq 0.15\,AU$ have a broad range of Ca II K emission while stars with distant planets ($a > 0.15\,AU$) have a narrow range of small Ca II K emission. Again, we distinguish between stars with planets discovered by the RV and transit methods. Significant fraction of close-in planets was discovered by the RV method. Apparently, some stars with close-in exoplanets (but not all of them) have high Ca II K emission. Unfortunately, this finding may be affected by selection biases (it is more difficult to detect distant planets around active stars).

To verify the above mentioned behaviour, we also explored the $\log R'_{HK}$ parameter as a function of the semi-major axis. This is illustrated in Figure 5. This figure also shows a clear distinction between the stars with close-in planets with semi-major axis less than 0.15 AU and stars with distant planets. Stars with close-in exoplanets generally have higher scatter in the $\log R'_{HK}$ values than stars with distant planets. This is mainly caused by hotter stars with transiting exoplanets. Once we concentrate only on cold stars with planets detected by the RV technique there might be a trend that stars with close-in planets have higher $\log R'_{HK}$ values than stars with distant planets but it is not as pronounced as in EQW measurements. At the same time, there is no strong correlation with the semi-major axis for $a \leq 0.15\,AU$.

However, what causes the high range of values of Ca II K emission for cold stars with close-in planets? Is it due to its dependence on time? If yes, on what timescales? On the timescale

of the planet orbital period, stellar activity cycle, age of the star or something else? Is there any other parameter/process which affects the stellar chromosphere? We explored whether it may be due to the eccentricity of the orbit but we did not find any convincing evidence for the eccentricity effect. If there is a dependence of the Ca II K emission on the semi-major axis of the planet, there ought to be some dependence on the mass m_p of the planet (or its magnetic field) as well. This dependence would have to be continuously reduced in case of sufficiently small planets. Unfortunately, we know only $m_p \sin i$ for most of the extrasolar planets. Nevertheless, we select all stars with temperatures $T \leq 5\,500\,K$ and with semi-major axis $a \leq 0.15\,AU$ and fit EQWs of the Ca II K emission by the following function:

$$W(m_p, T_{eff}) = aT_{eff} + b\log(m_p \sin i) + c \qquad (1)$$

We found the following coefficients: $a = 3.65 \times 10^{-3} \pm 5.7 \times 10^{-4}, b = -0.392 \pm 0.097, c = -20.4 \pm 2.9$. The a coefficient is significant beyond 6σ and temperature dependence is thus very clear. However, the b coefficient is also significant beyond 4σ and it indicates the statistically significant correlation of the chromospheric activity with the mass of the planet. We applied statistical F-test to justify the usage of additional parameter (planet mass) in the above mentioned fitting procedure. The test shows that the significance of the 3-parameter fit (equation (1)) over the 2-parameter fit $W(T_{eff}) = aT_{eff} + c$ is 0.003, which is below the common 0.05 value (2σ).

The above mentioned results are illustrated in Figure 6 where we plot the modified equivalent width of the Ca II K emission as a function of $m_p \sin i$. Stars with planets detected by RV and transit methods are marked with empty and full triangles respectively. Modified equivalent width is EQW corrected for the strong temperature dependence, namely $EQW - aT_{eff} - c$. Lower values mean larger emission and thus more massive planets show more activity of the host star. Unfortunately, this correlation might also be affected by the selection effect that it is more difficult to detect a less massive planet around a more active star.

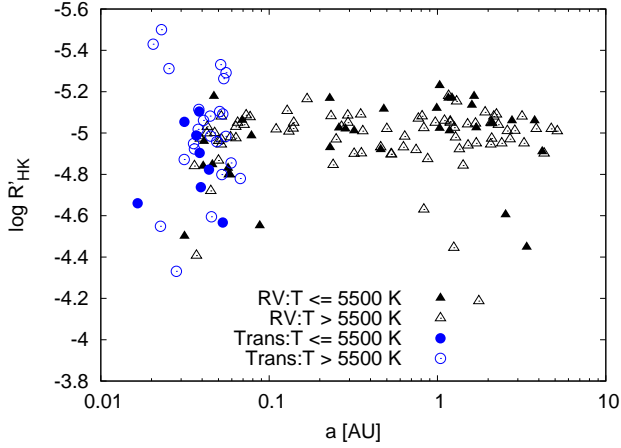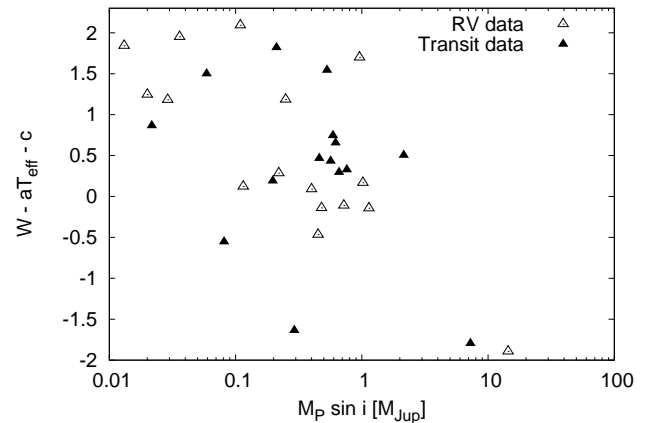**Fig. 6.** Dependence of the modified equivalent width of Ca II K emission on planet mass. Only stars with $T_{eff} \leq 5\,500\,K$ and $a \leq 0.15\,AU$ are considered. Modified equivalent width is equivalent width corrected for strong temperature dependence. By definition, the EQW is negative for emission. Consequently, lower values mean a higher emission and a higher chromospheric activity. Chromospheric activity of stars with more massive planets is higher than in those with less massive planets. Empty triangles - stars with planets detected by the RV method, full triangles - transit method.
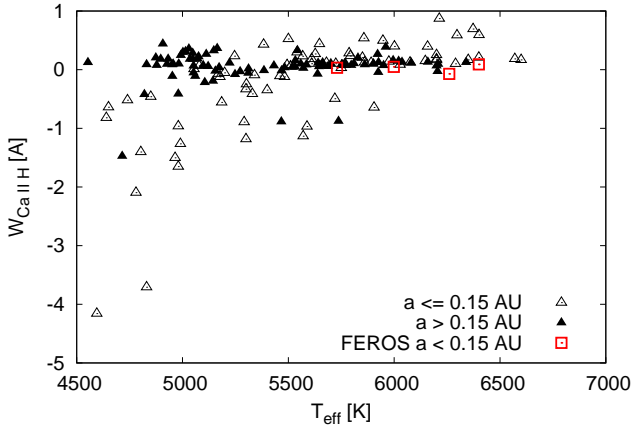
Fig. 7. Dependence of the equivalent width of Ca II H emission on the temperature of the star. Empty triangles are exoplanetary systems with $a \leq 0.15\,\mathrm{AU}$, full triangles are systems with $a > 0.15\,\mathrm{AU}$ and red squares are our data from FEROS.

Fig. 8. Dependence of the equivalent width of Ca II H emission on the semi-major axis. Empty triangles are exoplanetary systems discovered by RV technique, full triangles are systems discovered by transit method.

If our findings based on the Ca II K emission are true, than one can ask a question: how does this planet-star interaction work and why does it operate up to $a = 0.15\,\mathrm{AU}$? If it was caused by the tides of the planet, one would expect that the stellar activity would gradually decrease with a which may not be the case. We suggest that it may be due to the magnetic interaction which scales with the magnetic field of the planet. Magnetic field of the planet may be very sensitive to the rotation profile of the planet which is a subject to strong synchronization. Bodenheimer et al. (2001) suggested that exoplanets with semi-major axis $a \leq 0.15\,\mathrm{AU}$ are most probably synchronized.

4. Conclusions

We have found a statistically significant evidence that EQW of the Ca II K emission in the spectra of planet host stars as well as their $\log R'_{\mathrm{HK}}$ activity index depend on the semi-major axis of the exoplanet. Stars with close-in planets ($a \leq 0.15\,\mathrm{AU}$) have a generally higher Ca II K emission than stars with more distant planets. This means that a close-in planet may affect the level of the chromospheric activity of its host star and might heat the chromosphere of the star. This process operates up to the orbital period of about 20 days. Moreover, we have found a statistically significant evidence that the Ca II K emission of the host star (for $T_{\mathrm{eff}} \leq 5\,500\,\mathrm{K}$ and $a \leq 0.15\,\mathrm{AU}$) increases with the mass of the planet. The above mentioned trends may be affected by selection effects and should be revisited when less biased sample of stars with planets becomes available.

References

Bodenheimer, P., Lin, D. N. C., & Mardling, R. A. 2001, ApJ, 548, 466
Burrows, A., Budaj, J., & Hubeny, I. 2008, ApJ, 678, 1436
Burrows, A., Hubeny, I., Budaj, J., & Hubbard, W. B. 2007, ApJ, 661, 502
Canto Martins, B. L., Das Chagas, M. L., Alves, S., et al. 2011, A&A, 530, A73+
Cuntz, M., Saar, S. H., & Musielak, Z. E. 2000, ApJ, 533, L151
Fortney, J. J., Lodders, K., Marley, M. S., & Freedman, R. S. 2008, ApJ, 678, 1419
Gonzalez, G. 2011, MNRAS, 416, L80
Guillot, T. & Showman, A. P. 2002, A&A, 385, 156
Hartman, J. D. 2010, ApJ, 717, L138
Hubbard, W. B., Hattori, M. F., Burrows, A., Hubeny, I., & Sudarsky, D. 2007, Icarus, 187, 358
Hubeny, I., Burrows, A., & Sudarsky, D. 2003, ApJ, 594, 1011
Ip, W.-H., Kopp, A., & Hu, J.-H. 2004, ApJ, 602, L53
Isaacson, H. & Fischer, D. 2010, ApJ, 725, 875
Jordán, A. & Bakos, G. Á. 2008, ApJ, 685, 543
Kashyap, V. L., Drake, J. J., & Saar, S. H. 2008, ApJ, 687, 1339
Knutson, H. A., Howard, A. W., & Isaacson, H. 2010, ApJ, 720, 1569
Lanza, A. F. 2008, A&A, 487, 1163
Noyes, R. W., Hartmann, L. W., Baliunas, S. L., Duncan, D. K., & Vaughan, A. H. 1984, ApJ, 279, 763
Poppenhaeger, K. & Schmitt, J. H. M. M. 2011, ApJ, 735, 59
Rubenstein, E. P. & Schaefer, B. E. 2000, ApJ, 529, 1031
Saar, S. H., Cuntz, M., Kashyap, V. L., & Hall, J. C. 2008, in IAU Symposium, Vol. 249, IAU Symposium, ed. Y.-S. Sun, S. Ferraz-Mello, & J.-L. Zhou, 79–81
Shkolnik, E., Bohlender, D. A., Walker, G. A. H., & Collier Cameron, A. 2008, ApJ, 676, 628
Shkolnik, E., Walker, G. A. H., Bohlender, D. A., Gu, P., & Kürster, M. 2005, ApJ, 622, 1075
Vidal-Madjar, A., Lecavelier des Etangs, A., Désert, J.-M., et al. 2003, Nature, 422, 143
Wilson, O. C. 1968, ApJ, 153, 221
Wright, J. T., Marcy, G. W., Butler, R. P., & Vogt, S. S. 2004, ApJS, 152, 261
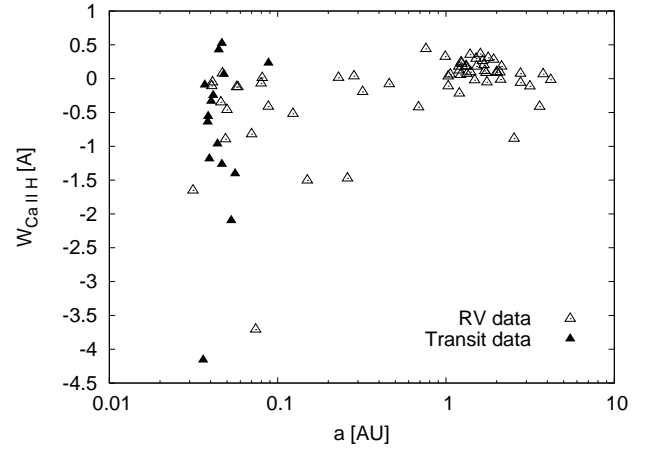
Table 1. Parameters of exoplanetary systems. Data taken from `http://www.exoplanet.eu/`. Systems below the line at the bottom part of the table describe our FEROS data sample.

Object	$M_p \sin i$ [M$_{Jup}$]	P_{orb} [days]	a [AU]	T_{eff} [K]	$W_{Ca II K}$ [Å]	$\log R'_{HK}$	Detection method
WASP-19 b	1.168	0.78884	0.01655	5500	-	-4.66	T
Kepler-10 b	0.0143	0.837495	0.01684	5627	0.1864	-	T
WASP-12 b	1.404	1.0914222	0.02293	6300	-	-5.5	T
HAT-P-23 b	2.09	1.212884	0.0232	5905	-0.7840	-	T
TrES-3	1.91	1.30618608	0.0226	5720	-0.7795	-4.549	T
CoRoT-1 b	1.03	1.5089557	0.0254	5950	-	-5.312	T
CoRoT-2 b	3.31	1.7429964	0.0281	5625	-	-4.331	T
WASP-3 b	2.06	1.8468372	0.0313	6400	0.1073	-4.872	T
HD 86081 b	1.5	2.1375	0.039	6028	0.0371	-4.973	RV
HAT-P-32 b	0.941	2.150009	0.0344	6001	0.4073	-	T
WASP-2 b	0.847	2.15222144	0.03138	5150	-	-5.054	T
HAT-P-7 b	1.8	2.2047298	0.0379	6350	0.1946	-5.018	T
HD 189733 b	1.138	2.21857312	0.03142	4980	-2.3605	-4.501	RV
WASP-14 b	7.341	2.2437661	0.036	6475	-	-4.923	T
TrES-2	1.253	2.470614	0.03556	5850	0.2015	-4.949	T
WASP-1 b	0.86	2.5199464	0.0382	6200	0.1785	-5.114	T
HD 73256 b	1.87	2.54858	0.037	5570	-1.6362	-4.407	RV
XO-2 b	0.62	2.615838	0.0369	5340	-0.2480	-4.988	T
HAT-P-16 b	4.193	2.77596	0.0413	6158	0.1982	-	T
HAT-P-5 b	1.06	2.788491	0.04075	5960	-	-5.061	T
HAT-P-20 b	7.246	2.875317	0.0361	4595	-5.4172	-	T
HD 149026 b	0.356	2.8758916	0.04288	6147	0.0581	-5.030	RV
HAT-P-3 b	0.591	2.899703	0.03866	5185	-0.7236	-4.904	T
HD 83443 b	0.4	2.985625	0.0406	5460	-0.3757	-4.84	RV
HD 46375 b	0.249	3.024	0.041	5199	-0.2325	-4.96	RV
TrES-1	0.761	3.0300722	0.0393	5300	-0.7222	-4.738	T
HAT-P-27 b/WASP-40 b	0.66	3.0395721	0.0403	5300	-0.7542	-	T
HAT-P-4 b	0.68	3.0565114	0.0446	5860	0.0739	-5.082	T
HAT-P-8 b	1.34	3.07632402	0.0449	6200	0.1113	-4.985	T
HD 187123 b	0.52	3.0965828	0.0426	5714	-	-4.999	RV
XO-3 b	11.79	3.1915239	0.0454	6429	-	-4.595	T
HAT-P-22 b	2.147	3.21222	0.0414	5302	-0.5378	-	T
HAT-P-12 b	0.211	3.2130598	0.0384	4650	-1.6008	-5.104	T
Kepler-4 b	0.077	3.21346	0.0456	5857	0.3420	-	T
Kepler-6 b	0.669	3.234723	0.04567	5647	0.4951	-	T
HAT-P-28 b	0.626	3.257215	0.0434	5680	0.2449	-	T
HAT-P-24 b	0.685	3.35524	0.0465	6373	0.8322	-	T
HD 88133 b	0.22	3.416	0.047	5494	-0.0570	-5.178	RV
HAT-P-33 b	0.763	3.474474	0.0503	6401	0.5521	-	T
BD-10 3166 b	0.48	3.487	0.046	5400	-0.8254	-4.847	RV
Kepler-18 b	0.0217	3.504725	0.0447	5383	0.1184	-	T
Kepler-8 b	0.603	3.52254	0.0483	6213	0.6870	-	T
HD 209458 b	0.714	3.52474859	0.04747	6075	0.0744	-5.00	RV
Kepler-5 b	2.114	3.54846	0.05064	6297	0.6038	-	T
TrES-4	0.917	3.5539268	0.05084	6200	0.1783	-5.104	T
HAT-P-25 b	0.567	3.652836	0.0466	5500	0.1131	-	T
WASP-11/HAT-P-10 b	0.46	3.722469	0.0439	4980	-1.7503	-4.823	T
WASP-17 b	0.486	3.735438	0.0515	6550	-	-5.331	T
HD 219828 b	0.066	3.8335	0.052	5891	0.0604	-4.945	RV
HAT-P-6 b	1.057	3.853003	0.05235	6570	0.1397	-4.799	T
HAT-P-9 b	0.67	3.922814	0.053	6350	-	-5.092	T
XO-1 b	0.9	3.9415128	0.0488	5750	-0.0056	-4.958	T
HAT-P-19 b	0.292	4.008778	0.0466	4990	-3.8168	-	T
HD 102195 b	0.45	4.113775	0.049	5291	-1.5490	-	RV
HAT-P-21 b	4.063	4.124461	0.0494	5588	-1.6625	-	T
XO-4 b	1.72	4.1250823	0.0555	5700	-	-5.292	T
HD 125612 c	0.058	4.1547	0.05	5897	-	-4.867	RV
XO-5 b	1.077	4.1877537	0.0487	5510	0.0093	-	T
61 Vir b	0.016	4.215	0.050201	5531	-	-4.962	RV
51 Peg b	0.468	4.23077	0.052	5793	0.0432	-5.08	RV

HAT-P-26 b	0.059	4.234516	0.0479	5079	-0.3556	-	T
WASP-13 b	0.485	4.353011	0.05379	5826	-	-5.263	T
Kepler-12 b	0.431	4.4379637	0.0556	5947	0.4331	-	T
HAT-P-1 b	0.524	4.4652934	0.05535	5975	0.1351	-4.984	T
ups And b	0.69	4.617136	0.059	6212	-	-4.980	RV
HAT-P-14 b	2.2	4.627657	0.0594	6600	0.1183	-4.855	T
HD 156668 b	0.0131	4.646	0.05	4850	-0.8485	-	RV
HAT-P-11 b	0.081	4.887804	0.053	4780	-3.4991	-4.567	T
HD 49674 b	0.115	4.9437	0.058	5482	-0.2634	-4.80	RV
HD 109749 b	0.28	5.24	0.0635	5610	0.0512	-4.975	RV
HD 7924 b	0.029	5.3978	0.057	5177	-0.3167	-4.83	RV
HAT-P-18 b	0.197	5.508023	0.0559	4803	-2.6726	-	T
HAT-P-2 b	8.74	5.6334729	0.0674	6290	0.0552	-4.78	T
HD 1461 b	0.0239	5.7727	0.063438	5765	0.0179	-5.03	RV
HD 68988 b	1.9	6.276	0.071	5767	0.0495	-5.04	RV
HD 168746 b	0.23	6.403	0.065	5610	0.0273	-5.05	RV
HD 102956 b	0.96	6.495	0.081	5054	-0.2472	-	RV
HIP 14810 b	3.88	6.673855	0.0692	5485	-	-5.062	RV
HD 185269 b	0.94	6.838	0.077	5980	-	-5.077	RV
HD 217107 b	1.33	7.12689	0.073	5666	-	-5.086	RV
HIP 57274 b	0.036	8.1352	0.07	4640	-1.5066	-	RV
HD 162020 b	14.4	8.428198	0.074	4830	-4.6563	-	RV
HD 69830 b	0.033	8.667	0.0785	5385	-	-4.987	RV
Kepler-19 b	0.064	9.2869944	0.118	5541	0.1498	-	T
HD 97658 b	0.02	9.4957	0.0797	5170	-0.2781	-	RV
HAT-P-17 b	0.53	10.338523	0.0882	5246	0.2963	-	T
HD 130322 b	1.02	10.72	0.088	5330	-0.7721	-4.552	RV
HAT-P-15 b	1.946	10.863502	0.0964	5568	0.0856	-	T
HD 38529 b	0.78	14.3104	0.131	5697	-	-5.007	RV
HD 179079 b	0.08	14.476	0.11	5724	0.0267	-5.018	RV
HD 99492 b	0.109	17.0431	0.1232	4740	-0.9996	-	RV
HD 190360 c	0.057	17.1	0.128	5588	-	-5.107	RV
HD 16417 b	0.069	17.24	0.14	5936	-	-5.050	RV
HD 33283 b	0.33	18.179	0.168	5995	0.1073	-5.164	RV
HD 195019 b	3.7	18.20163	0.1388	5787	0.1036	-5.022	RV
HD 192263 b	0.72	24.348	0.15	4965	-2.3811	-	RV
HD 224693 b	0.71	26.73	0.233	6037	0.0726	-5.082	RV
HD 43691 b	2.49	36.96	0.24	6200	0.0103	-4.846	RV
HD 11964 c	0.079	37.91	0.229	5248	-	-5.168	RV
HD 45652 b	0.47	43.6	0.23	5312	-0.2185	-4.930	RV
HD 107148 b	0.21	48.056	0.269	5797	0.0290	-5.03	RV
HD 90156 b	0.057	49.77	0.25	5599	-	-4.969	RV
HD 74156 b	1.88	51.65	0.294	5960	-	-5.050	RV
HD 37605 b	2.84	55.23	0.26	5475	-	-5.025	RV
HD 168443 b	7.659	58.11247	0.2931	5591	-	-5.085	RV
HD 85512 b	0.011	58.43	0.26	4715	-2.6150	-	RV
HD 3651 b	0.2	62.23	0.284	5173	-0.2119	-5.02	RV
HD 178911 B b	6.292	71.487	0.32	5650	-	-4.900	RV
Gl 785 b	0.053	74.72	0.32	5144	-0.4055	-5.011	RV
HD 163607 b	0.77	75.229	0.36	5543	0.0947	-5.009	RV
HD 16141 b	0.215	75.82	0.35	5533	0.0657	-5.09	RV
HD 114762 b	10.98	83.9151	0.353	5934	-	-4.902	RV
HD 80606 b	3.94	111.43637	0.449	5645	-0.0441	-	RV
70 Vir b	6.6	116.67	0.48	5432	-	-5.116	RV
HD 216770 b	0.65	118.45	0.46	5248	-0.3098	-4.92	RV
HD 52265 b	1.05	119.6	0.5	6159	0.1133	-5.02	RV
HD 102365 b	0.05	122.1	0.46	5650	0.0863	-4.931	RV
HD 231701 b	1.08	141.6	0.53	6208	0.0829	-4.897	RV
HD 37124 b	0.675	154.378	0.53364	5610	-	-4.897	RV
HD 11506 c	0.82	170.46	0.639	6058	-	-4.983	RV
HD 5891 b	7.6	177.11	0.76	4907	-0.0017	-	RV
HD 155358 b	0.89	195	0.628	5760	-	-4.931	RV
HD 82943 c	2.01	219	0.746	5874	-	-4.918	RV
HD 218566 b	0.21	225.7	0.6873	4820	-1.0175	-	RV

HD 8574 b	2.11	227.55	0.77	6080	0.1015	-5.07	RV
HD 134987 b	1.59	258.19	0.81	5740	-	-5.081	RV
HD 40979 b	3.28	263.1	0.83	6205	-0.2931	-4.63	RV
HD 12661 b	2.3	263.6	0.83	5742	-	-5.024	RV
HD 164509 b	0.48	282.4	0.875	5922	0.2167	-4.874	RV
HD 175541 b	0.61	297.3	1.03	5060	-0.2814	-5.23	RV
HD 92788 b	3.86	325.81	0.97	5559	0.0118	-5.05	RV
HD 33142 b	1.3	326.6	1.06	5052	-0.2125	-	RV
HD 192699 b	2.5	351.5	1.16	5220	-	-5.169	RV
HD 4313 b	2.3	356	1.19	5035	-0.2078	-	RV
HD 96063 b	0.9	361.1	0.99	5148	-0.0725	-5.120	RV
HD 212771 b	2.3	373.3	1.22	5121	-0.1416	-5.170	RV
alf Ari b	1.8	380.8	1.2	4553	-0.4053	-	RV
HD 28185 b	5.7	383	1.03	5482	0.0092	-5.023	RV
HD 28678 b	1.7	387.1	1.24	5076	0.1876	-	RV
HD 75898 b	2.51	418.2	1.19	6021	0.0944	-5.056	RV
HD 4203 b	2.07	431.88	1.164	5701	0.0444	-5.18	RV
HD 1502 b	3.1	431.8	1.31	5049	-0.0948	-	RV
HD 98219 b	1.8	436.9	1.23	4992	-0.1541	-	RV
HD 99109 b	0.502	439.3	1.105	5272	-0.1254	-5.06	RV
HD 210277 b	1.23	442.1	1.1	5532	-0.0307	-5.06	RV
HD 108863 b	2.6	443.4	1.4	4956	-0.0677	-	RV
24 Sex b	1.99	452.8	1.333	5098	-0.186	-	RV
HD 188015 b	1.26	456.46	1.19	5520	-0.0296	-5.05	RV
HD 136418 b	2	464.3	1.32	5071	-0.0939	-	RV
HD 31253 b	0.5	466	1.26	5960	0.1123	-5.026	RV
HD 180902 b	1.6	479	1.39	5030	0.3773	-	RV
HD 96167 b	0.68	498.9	1.3	5770	0.0629	-5.153	RV
HD 20367 b	1.07	500	1.25	6128	-	-4.445	RV
HD 114783 b	1.0	501	1.2	5105	-0.5261	-	RV
HD 95089 b	1.2	507	1.51	5002	-0.1224	-	RV
HD 158038 b	1.8	521	1.52	4897	-0.4858	-	RV
HD 192310 c	0.075	525.8	1.18	5166	-	-5.011	RV
HD 4113 b	1.56	526.62	1.28	5688	-0.0128	-4.979	RV
HD 19994 b	1.68	535.7	1.42	5984	-	-4.843	RV
HD 222582 b	7.75	572.38	1.35	5662	0.0567	-4.922	RV
HD 206610 b	2.2	610	1.68	4874	-0.2457	-	RV
HD 200964 b	1.85	613.8	1.601	5164	-0.1220	-5.135	RV
HD 183263 b	3.67	626.5	1.51	5888	-	-5.042	RV
HD 141937 b	9.7	653.22	1.52	5925	-0.1438	-4.94	RV
HD 181342 b	3.3	663	1.78	5014	-0.0290	-	RV
HD 116029 b	2.1	670.2	1.73	4951	-0.4563	-	RV
HD 5319 b	1.94	675	1.75	5052	-0.3424	-	RV
HD 152581 b	1.5	689	1.48	5155	0.0610	-	RV
HD 38801 b	10.7	696.3	1.7	5222	-0.1931	-5.026	RV
HD 82886 b	1.3	705	1.65	5112	0.0341	-5.178	RV
HD 18742 b	2.7	772	1.92	5048	-0.2086	-	RV
HD 102329 b	5.9	778.1	2.01	4830	-0.5418	-	RV
16 Cyg B b	1.68	799.5	1.68	5766	-	-5.046	RV
HD 4208 b	0.8	829	1.7	5571	0.0141	-4.95	RV
HD 70573 b	6.1	851.8	1.76	5737	-1.2001	-4.187	RV
HD 99706 b	1.4	868	2.14	4932	-0.2245	-	RV
HD 131496 b	2.2	883	2.09	4927	-0.2836	-	RV
HD 45350 b	1.79	890.76	1.92	5754	0.0338	-5.10	RV
HD 30856 b	1.8	912	2	4982	-0.2822	-	RV
HD 16175 b	4.4	990	2.1	6000	-	-5.048	RV
HD 34445 b	0.79	1049	2.07	5836	-	-4.945	RV
HD 10697 b	6.38	1076.4	2.16	5641	-0.0343	-5.08	RV
47 Uma b	2.53	1078	2.1	5892	-	-4.973	RV
HD 114729 b	0.84	1135	2.08	5662	0.0658	-5.05	RV
HD 170469 b	0.67	1145	2.24	5810	0.0452	-5.09	RV
HD 164922 b	0.36	1155	2.11	5385	-0.1236	-5.05	RV
HD 30562 b	1.29	1157	2.3	5861	0.0667	-5.04	RV
HD 126614 b	0.38	1244	2.35	5585	0.0434	-	RV

HD 50554 b	5.16	1293	2.41	5902	0.0535	-4.95	RV
HD 142245 b	1.9	1299	2.77	4878	-0.2781	-	RV
HD 196885 A b	2.98	1326	2.6	6340	0.1021	-5.01	RV
HD 171238 b	2.6	1523	2.54	5467	-1.3506	-4.605	RV
HD 23596 b	8.1	1565	2.88	5888	-	-5.011	RV
HD 106252 b	7.56	1600	2.7	5754	0.0617	-4.97	RV
14 Her b	4.64	1773.4	2.77	5311	-0.1555	-5.06	RV
HD 73534 b	1.15	1800	3.15	4952	-0.4324	-	RV
HD 66428 b	2.82	1973	3.18	5752	0.0465	-5.08	RV
HD 89307 b	1.78	2157	3.27	5950	0.0688	-4.95	RV
HD 50499 b	1.71	2482.7	3.86	5902	0.1008	-5.02	RV
eps Eri b	1.55	2502	3.39	5116	-	-4.448	RV
HD 117207 b	2.06	2627.08	3.78	5432	0.0276	-5.06	RV
HD 87883 b	1.78	2754	3.6	4980	-0.6913	-	RV
HD 106270 b	11	2890	4.3	5638	-0.2846	-4.901	RV
HD 154345 b	0.947	3340	4.19	5468	-0.1824	-4.91	RV
HD 72659 b	3.15	3658	4.74	5926	0.0844	-5.02	RV
HD 13931 b	1.88	4218	5.15	5829	0.1010	-5.009	RV
HD 149143 b	1.36	4.088	0.052	5730	0.0716	-4.97	RV
HD 179949 b	0.95	3.0925	0.045	6260	0.0678	-4.72	RV
HD 212301 b	0.45	2.245715	0.036	5998	0.0966	-4.84	RV
WASP-18 b	10.43	0.9414518	0.02047	6400	0.2145	-5.43	T